JCI The Journal of Clinical Investigation

Rare codons capacitate *Kras*-driven de novo tumorigenesis

Nicole L.K. Pershing, … , David M. MacAlpine, Christopher M. Counter

J Clin Invest. 2015;125(1):222-233. https://doi.org/10.1172/JCI77627.

Research Article **Oncology**

The *KRAS* gene is commonly mutated in human cancers, rendering the encoded small GTPase constitutively active and oncogenic. This gene has the unusual feature of being enriched for rare codons, which limit protein expression. Here, to determine the effect of the rare codon bias of the *KRAS* gene on de novo tumorigenesis, we introduced synonymous mutations that converted rare codons into common codons in exon 3 of the *Kras* gene in mice. Compared with control animals, mice with at least 1 copy of this $Kras^{ex3op}$ allele had fewer tumors following carcinogen exposure, and this allele was mutated less often, with weaker oncogenic mutations in these tumors. This reduction in tumorigenesis was attributable to higher expression of the $Kras^{ex3op}$ allele, which induced growth arrest when oncogenic and exhibited tumor-suppressive activity when not mutated. Together, our data indicate that the inherent rare codon bias of *KRAS* plays an integral role in tumorigenesis.

Rare codons capacitate *Kras*-driven de novo tumorigenesis

Nicole L.K. Pershing,[1] Benjamin L. Lampson,[1] Jason A. Belsky,[1] Erin Kaltenbrun,[1] David M. MacAlpine,[1] and Christopher M. Counter[1,2]

[1]Department of Pharmacology and Cancer Biology and [2]Department of Radiation Oncology, Duke University Medical Center, Durham, North Carolina, USA.

The *KRAS* gene is commonly mutated in human cancers, rendering the encoded small GTPase constitutively active and oncogenic. This gene has the unusual feature of being enriched for rare codons, which limit protein expression. Here, to determine the effect of the rare codon bias of the *KRAS* gene on de novo tumorigenesis, we introduced synonymous mutations that converted rare codons into common codons in exon 3 of the *Kras* gene in mice. Compared with control animals, mice with at least 1 copy of this $Kras^{ex3op}$ allele had fewer tumors following carcinogen exposure, and this allele was mutated less often, with weaker oncogenic mutations in these tumors. This reduction in tumorigenesis was attributable to higher expression of the $Kras^{ex3op}$ allele, which induced growth arrest when oncogenic and exhibited tumor-suppressive activity when not mutated. Together, our data indicate that the inherent rare codon bias of *KRAS* plays an integral role in tumorigenesis.

Introduction

The mammalian RAS family of small GTPases is composed of 3 genes that encode the proteins HRAS, NRAS, KRAS4A, and KRAS4B, the latter 2 being derived from alternatively spliced transcripts. RAS proteins transmit signals from surface receptors to intracellular signaling proteins. Upon receptor activation, guanine nucleotide exchange factors (GEFs) accelerate the exchange of GDP for GTP on RAS, which stabilizes an altered conformation that fosters binding and activation of effector proteins. In turn, GTPase–activating proteins (GAPs) increase the GTPase activity of RAS, returning the proteins to the inactive GDP-bound conformation. In a quarter or more of human cancers, one of the *RAS* genes has an activating or oncogenic mutation. These mutations typically occur at G12, G13, or Q61, with the frequency of each mutation in each *RAS* gene differing between cancers. While the underlying defect of mutations differs, each results in sustained GTP binding and RAS activation. Oncogenic RAS proteins chronically activate MAPK, PI3K, RAL, and other effector pathways to promote tumorigenesis (reviewed in refs. 1, 2).

The 4 RAS proteins share 79% amino acid sequence identity, with most of the variability residing in the last 25 amino acids that encode sites of different posttranslational modifications (3). The nucleotide sequences of the genes are, however, more divergent (4). Nucleotide differences often occur at the third, or wobble, position of the codon (5). In this regard, *KRAS* is preferentially encoded by A or T at wobble base pairs, *HRAS* by G or C, and *NRAS* by an intermediate mixture of nucleotides (4). Mammalian codons ending in A or T are less represented, or rare, in mammalian exomes (6). The functional significance of rare codons in transcripts of higher eukaryotes is poorly understood (5). Nevertheless, discordance in codon usage between genomes of different species can result in poor translation in heterologous systems (e.g., ref. 7). Rare codons can also reduce the efficiency of translation elongation, with functional consequences in other organisms (e.g., ref. 8). Similarly, we have previously demonstrated that rare codons impede *KRAS* translation, reducing protein expression relative to that of the other RAS isoforms (4). However, the consequences of altering codon usage within an endogenous gene have not been tested in mammalian organisms.

Oncogenic "driver" mutations in *KRAS* initiate the conversion of normal cells to a tumorigenic state (1). Paradoxically, oncogenic RAS, through activation of the MAPK pathway, can also induce senescent growth arrest in primary cells (9). One factor influencing this divergent response is the expression level of oncogenic RAS itself, with high expression inducing senescence and low expression promoting hyperplasia in vivo (10). The rare codon bias of *KRAS* has not been assessed with regard to tumor initiation, a process critically sensitive to RAS protein levels. Thus, we evaluated the effect of converting rare codons into common codons in the endogenous mouse *Kras* gene on in vivo carcinogenesis.

Results

Creation of mice with a codon-altered Kras allele. To investigate the influence of rare codons in *Kras* in vivo, a knock-in approach was designed to minimally perturb the murine *Kras* gene while maximally altering codon bias. Specifically, converting rare codons into common codons in exon 3 increased ectopic KRAS protein expression more, for reasons that remain to be elucidated, than did similar alternations to exons 1 or 2 (Figure 1A). Thus, we designed a knock-in construct to introduce 33 synonymous mutations into murine *Kras* exon 3 that optimized (*ex3op*) 27 rare codons by converting them into more common codons, thereby increasing common codon usage (Figure 1, B–D, and Supplemental Figure 1; supplemental material available online with this article;

Note regarding evaluation of this manuscript: Manuscripts authored by scientists associated with Duke University, The University of North Carolina at Chapel Hill, Duke-NUS, and the Sanford-Burnham Medical Research Institute are handled not by members of the editorial board but rather by the science editors, who consult with selected external editors and reviewers.

Conflict of interest: The authors have declared that no conflict of interest exists.

Submitted: June 19, 2014; **Accepted:** October 30, 2014.

Reference information: *J Clin Invest*. 2015;125(1):222–233. doi:10.1172/JCI77627.

doi:10.1172/JCI77627DS1). Heterozygous *Kras*$^{ex3op(neo)}$ mice, identified by genotyping PCR that yielded the expected 388-bp product (Figure 1, D and E), were crossed with C57BL6/J-*CMV-Cre* or, to maintain a 129 background, with 129S/Sv-*PRM-Cre* transgenic mice to induce Cre-mediated recombination between *loxP* sites and delete the *neo* cassette. Successful excision of the *neo* cassette in the resulting offspring was identified by PCR amplification of genomic DNA, yielding the expected 504-bp product (Figure 1, D and E).

To determine the impact of converting rare codons into common codons on endogenous KRAS mRNA and protein levels, SV40-immortalized mouse embryonic fibroblasts (MEFs) were generated from littermates homozygous for the *ex3op* or native *Kras* alleles. Semiquantitative reverse transcription PCR (RT-PCR) revealed no overt difference in total *Kras* mRNA expression levels between *Kras*$^{ex3op/ex3op}$ and *Kras*$^{nat/nat}$ MEFs. We also observed no obvious differences in the levels of *Kras4a* and *Kras4b* splice forms (Figure 1F), an important consideration, given that synonymous mutations can alter splicing of oncogenes (11) and that both splice forms of *Kras* are known to contribute to tumorigenesis (12, 13). While mRNA levels remained unchanged, immunoblot analysis revealed roughly 2-fold more endogenous KRAS protein in *Kras*$^{ex3op/ex3op}$ MEFs compared with that detected in *Kras*$^{nat/nat}$ MEFs (Figure 1G). Finally, although we observed considerable variability between mice of the same genotype (data not shown), immunoblot comparisons of 16 individual age-matched pairs revealed, on average, more endogenous KRAS protein in lung tissue from *Kras*$^{ex3op/ex3op}$ mice compared with that from *Kras*$^{nat/nat}$ mice (Figure 1H). Thus, 33 synonymous point mutations in exon 3 of the murine *Kras* gene resulting in the conversion of 27 rare codons to common codons increased the average amount of KRAS protein detected in the tested cells and tissues.

Kras$^{ex3op/ex3op}$ *mice have no overt developmental phenotype*. To investigate the developmental consequences of changing *Kras* codon bias, *Kras*$^{ex3op/nat}$ mice were crossed and the frequency of offspring with each of 3 possible genotypes assessed. Of 295 offspring, we observed no difference from the expected Mendelian ratios of *Kras*$^{nat/nat}$, *Kras*$^{ex3op/nat}$, and *Kras*$^{ex3op/ex3op}$ mice (Supplemental Table 1). The animals also had no obvious physical or reproductive abnormalities (data not shown), and we noted no significant differences in weight between adult *Kras*$^{nat/nat}$ and *Kras*$^{ex3op/ex3op}$ mice, regardless of age or strain background (Supplemental Figure 2). To investigate the *Kras*^{ex3op} allele in a background sensitive to decreased *Kras* gene dosage, we assessed the postnatal development of chylous ascites. Chylous ascites arises in *Kras*$^{+/-}$ mice on either an *Hras*$^{-/-}$ or *Nras*$^{-/-}$ background, and the incidence of this phenotype is inversely correlated with the number of functional *Ras* alleles (14). Thus, *Kras*$^{ex3op/nat}$ *Nras*$^{-/-}$ *Hras*$^{-/-}$ mice were crossed and 121 offspring evaluated. Again, we observed no significant differences from the expected Mendelian ratios of offspring, and the incidence of chylous ascites was not significantly different between the 3 *Kras* genotypes (Supplemental Tables 2 and 3). Hence, the *Kras*^{ex3op} allele appears developmentally equivalent to the native *Kras* allele.

Kras$^{ex3op/nat}$ *mice develop fewer lung tumors following carcinogen exposure*. To investigate the effect of the *Kras*^{ex3op} allele on tumorigenesis, mice were administered the chemical carcinogen urethane to induce lung adenomas characterized by Q61L or R oncogenic mutations in the *Kras* gene (15). To populate mice for this study, we crossed *Kras*$^{ex3op(neo)/nat}$ mice with *Kras*$^{nat/nat}$ mice containing the *CMV-Cre* transgene to excise the *neo* cassette used in the generation of the *Kras*$^{ex3op(neo)}$ allele (Figure 2A). We injected cohorts of *Kras*$^{ex3op/nat}$ *CMV-Cre* and *Kras*$^{nat/nat}$ *CMV-Cre* littermates with urethane at 6 to 8 weeks of age. Eleven to 12 months later, when tumor incidence was expected to be near 100% (16), the surviving mice were euthanized and their lungs removed to assess tumor number and size. We calculated the tumor burden (defined as the sum of tumor diameters) from these values. *Kras*$^{ex3op/nat}$ *CMV-Cre* mice exhibited a greater than 2-fold decrease in tumor burden compared with that observed in their *Kras*$^{nat/nat}$ *CMV-Cre* littermates (Figure 2B). We observed no lung lesions in untreated mice of either genotype (data not shown). To ascertain the reproducibility of this effect at an earlier time point (9 months), we administered urethane to another independent cohort of *Kras*$^{ex3op/nat}$ *CMV-Cre* and *Kras*$^{nat/nat}$ *CMV-Cre* littermates. Mice carrying the *Kras*^{ex3op} allele again exhibited a greater than 2-fold reduction in tumor burden (Figure 2C). We confirmed the excision of the *neo* cassette in tested tumors arising in *Kras*$^{ex3op/nat}$ *CMV-Cre* mice and observed no obvious differences in tumor histology between cohorts (Supplemental Figure 3, A and B). Finally, to determine whether these results were reproducible between targeting events, *Kras*$^{ex3op(neo)2/nat}$ mice generated from an independently targeted embryonic stem (ES) cell clone were crossed with *Kras*$^{nat/nat}$ *CMV-Cre* mice. We injected the resultant *Kras*$^{ex3op2/nat}$ *CMV-Cre* and *Kras*$^{nat/nat}$ *CMV-Cre* littermates with urethane and analyzed them 9 months later for lung tumor burden. Again, we found that *Kras*$^{ex3op2/nat}$ *CMV-Cre* mice exhibited a nearly 4-fold reduction in tumor burden (Figure 2D). In all 3 experiments, the reduction in tumor burden was primarily a consequence of decreased tumor multiplicity and not tumor size, suggesting fewer successful tumor initiation events (Supplemental Figure 3, C–E). We also found no detectable difference between urethane-induced tumors arising in *Kras*$^{ex3op/nat}$ *CMV-Cre* and *Kras*$^{nat/nat}$ *CMV-Cre* mice in terms of Ki67 immunoreactivity, a marker of cell proliferation; TUNEL activity, a marker of cell death; or Nqo1 immunoreactivity, a protein reported to be part of the NRF2 antioxidant and cellular detoxification program induced by oncogenic *Kras* during pancreatic cancer (17), supportive of the *Kras*^{ex3op2} allele influencing early tumorigenesis (Supplemental Figure 3, F–H). Collectively, these data suggest that converting rare codons to common codons in *Kras* reduces the initiation of tumors induced by the carcinogen urethane.

Reduced Kras^{G12D}*-driven tumorigenesis in the presence of a nononcogenic Kras*^{ex3op} *allele*. The observed reduction in tumor burden in *Kras*$^{ex3op/nat}$ mice could be an effect of changing codon bias in the oncogenic or nononcogenic allele. Loss of 1 *Kras* allele can substantially increase sensitivity to urethane, suggesting that the nononcogenic (WT) *Kras* allele suppresses the tumorigenic activity of the oncogenic *Kras* allele (18). As such, increasing expression of the nononcogenic *Kras* allele, in this case by converting rare codons into common codons, could be expected to reduce urethane carcinogenesis (19). To directly test this possibility, we crossed B6 129S-*Kras*$^{ex3op/nat}$ mice with *Kras*$^{LSL-G12D/nat}$ mice from a mixed background, which harbor a Cre-inducible *Kras*$^{LSL-G12D}$

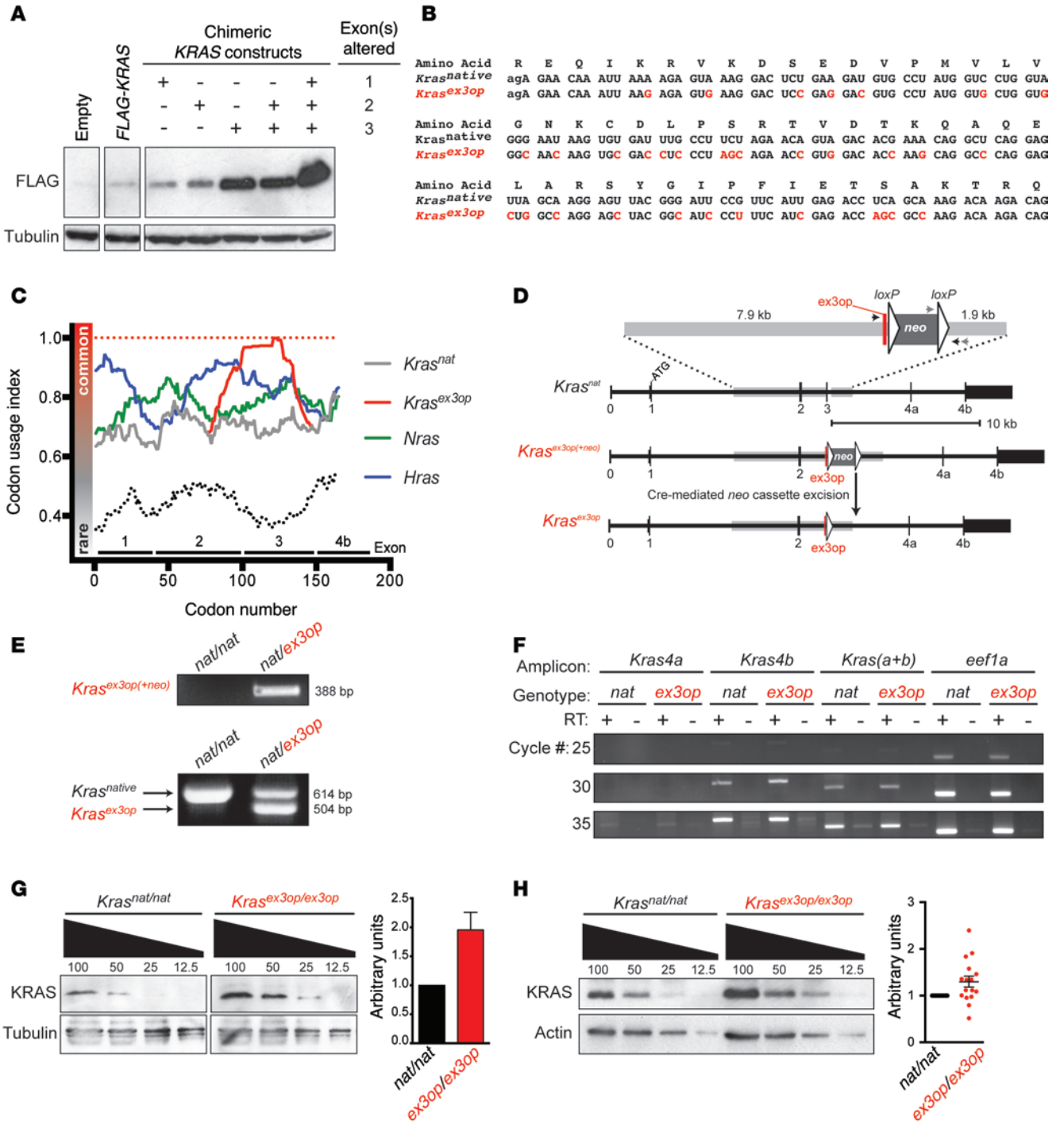

Figure 1. Generation and characterization of the *Kras*^{ex3op} allele. (**A**) Immunoblot reveals changing rare codons to common codons in exon 3 increases ectopic KRAS expression (1 of 2 experiments using cells independently transduced with expression vectors). (**B**) Position of synonymous mutations (red) in *Kras*^{ex3op} aligned to *Kras*^{nat} within exon 3. Lowercase letters denote nucleotides from exon 2. (**C**) Sliding window of codon usage index demonstrating the relative codon usage of the mouse *Ras* genes including the engineered enrichment of common codons in exon 3 of *Kras*^{ex3op} (red) relative to *Kras*^{nat} (gray). Theoretical *Kras* transcripts encoded by all common (red dotted line) or all rare (black dotted line) are plotted for reference. (**D**) Targeting strategy to change codon usage in exon 3 of *Kras*. Arrows indicate PCR primers used for genotyping. (**E**) Representative genotyping from mice with *Kras*^{nat} and/or *Kras*^{ex3op} alleles used in all genotyping experiments. (**F**) Semiquantitative RT-PCR analysis revealed similar levels of *Kras* splice forms *4a* and *4b* in MEFs isolated from *Kras*$^{ex3op/ex3op}$ versus those from *Kras*$^{nat/nat}$ mice (1 of 2 experiments using independently derived MEFs). (**G**) Representative example and quantification (mean ± SEM) of immunoblots revealed higher levels of KRAS protein in lysates of MEFs isolated from *Kras*$^{ex3op/ex3op}$ than levels detected in *Kras*$^{nat/nat}$ mice (1 of 2 experiments using independently-derived MEFs). (**H**) Representative example and quantification (mean ± SEM) of immunoblots revealed higher levels of KRAS protein in total lung lysates isolated from *Kras*$^{ex3op/ex3op}$ mice than those detected in *Kras*$^{nat/nat}$ mice. Comparisons were made using lysates from a total of 16 *Kras*$^{ex3op/ex3op}$ versus 16 *Kras*$^{nat/nat}$ mice.

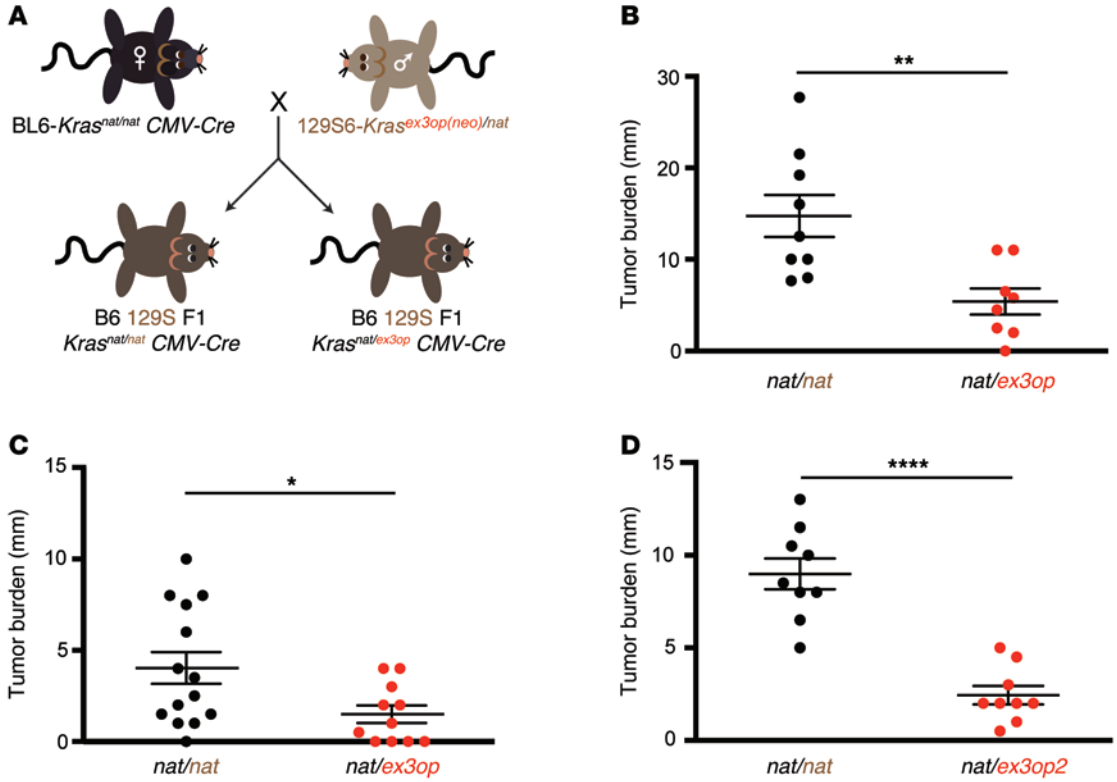

Figure 2. *Kras*$^{ex3op/nat}$ mice are resistant to urethane. (**A**) Strategy to generate *Kras*$^{ex3op/nat}$ *CMV-Cre* and *Kras*$^{nat/nat}$ *CMV-Cre* F1 mixed-background littermates for urethane carcinogenesis. (**B**–**D**) Reduction of tumor burden (mean ± SEM) in *Kras*$^{ex3op/nat}$ *CMV-Cre* versus *Kras*$^{nat/nat}$ *CMV-Cre* mice (**B**) 11–12 months ($n \geq 8$, $^{**}P < 0.01$) or (**C**) 9 months ($n \geq 11$, $^{*}P < 0.05$) after urethane administration and (**D**) *Kras*$^{ex3op/nat}$ *CMV-Cre* versus *Kras*$^{nat/nat}$ *CMV-Cre* mice generated from a second founder line 9 months after urethane administration ($n = 9$, $^{****}P < 0.0001$). *P* values were calculated by an unpaired, 2-tailed *t* test.

oncogenic allele (20). Cohorts of *Kras*$^{LSL-G12D/ex3op}$ and *Kras*$^{LSL-G12D/nat}$ littermates were administered adenovirus encoding Cre recombinase (AdCre) via intranasal inhalation to activate the oncogenic *Kras*$^{LSL-G12D}$ allele in lung epithelium and initiate lung tumorigenesis (Figure 3A). Four and 6 months later, mice were euthanized, the lungs removed, and tumor burden assessed. We found that AdCre-treated *Kras*$^{LSL-G12D/ex3op}$ mice exhibited at least a 2-fold reduction in tumor burden compared with that seen in control *Kras*$^{LSL-G12D/nat}$ mice at both time points (Figure 3, B and C). At the 4-month time point, this difference was primarily due to a reduction in tumor incidence, similar to what was was observed in the mice injected with urethane, but by 6 months, decreased lesion size was evident (Supplemental Figure 4, A and B). No overt differences in tumor histology were apparent between genotypes (Supplemental Figure 4C). With the caveat that the *Kras* alleles were not congenic (19), the *Kras*^{ex3op} allele more potently suppresses oncogenic *Kras*–driven lung tumor formation.

The Kras^{ex3op} *allele is less frequently mutated in urethane-induced lung tumors*. We next determined the difference in frequency and type of oncogenic mutations occurring in the *Kras*^{ex3op} and *Kras*^{nat} alleles inherited from the same parent. There are a number of SNPs in the *Kras* gene that differ between the 129S6/SvEvTac (termed 129 hereafter) background on which *Kras*^{ex3op} mice were generated and the C57BL6/J (termed BL6 hereafter) strain that carries the *CMV-Cre* transgene used to excise the *neo* cassette (Figure 4A and Supplemental Figure 5). We used these SNPs to identify the 129-*Kras*^{ex3op} or 129-*Kras*^{nat} allele from 1 parent and the remaining BL6-*Kras*^{nat} allele inherited from the other parent (Figure 2A and Supplemental Figure 5). RNA was isolated from tumors arising from the aforementioned *Kras*$^{ex3op/nat}$ *CMV-Cre* and *Kras*$^{nat/nat}$ *CMV-Cre* littermates injected with urethane from the 2 different founder lines (Figure 2, B and D) and RT-PCR amplified with primers specific for *Kras* (Figure 4A). The products were cloned into a plasmid vector, and individual inserts were sequenced. We sequenced 8–12 independent inserts from each tumor to identify (a) the strain (129 or BL6) based on SNPs, (b) the type of *Kras* allele (*nat* or *ex3op*) based on the exon 3 sequence, and (c) the presence of oncogenic mutations (Supplemental Table 4). As expected (15), we found that almost all tumors from *Kras*$^{nat/nat}$ *CMV-Cre* mice carried an oncogenic Q61L or R (Q61L/R) mutation. Consistent with the 129 strain being more susceptible to urethane mutagenesis than the BL6 strain (18), all oncogenic *Kras* mutations detected in tumors from these mice occurred in the 129-*Kras*^{nat} allele. In contrast, the percentage of tumors from *Kras*$^{ex3op/nat}$ *CMV-Cre* mice with a *Kras* oncogenic mutation occurring in the 129-*Kras*^{ex3op} allele was reduced by half. Moreover, instead of canonical Q61L/R mutations, we detected G12D mutations, which are rarely detected following urethane administration (21), in the 129-*Kras*^{ex3op} allele (Figure 4B). We observed no significant differences in the mutation spectrum between the 2 founder lines (Supplemental Table 4). To independently validate these results using a more sensitive assay, *Kras* mRNA from tumors of another cohort of mice injected

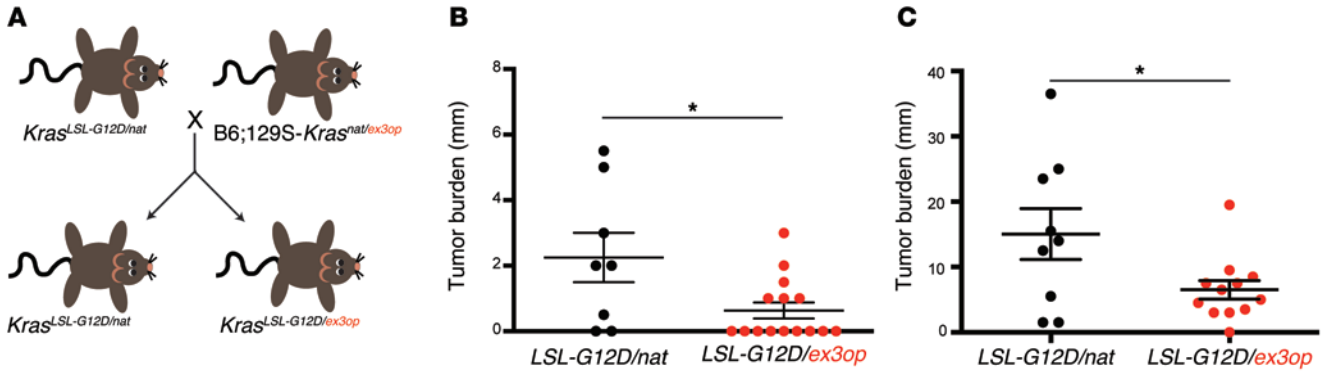

Figure 3. Increased resistance of $Kras^{ex3op}$ mice to lung tumorigenesis driven by $Kras^{G12D}$. (**A**) Strategy to generate $Kras^{LSL\text{-}G12D/ex3op}$ and $Kras^{LSL\text{-}G12D/nat}$ littermates for analysis of tumor burden. (**B** and **C**) Reduction of tumor burden (mean ± SEM) in $Kras^{LSL\text{-}G12D/ex3op}$ versus $Kras^{LSL\text{-}G12D/nat}$ mice (**B**) 4 months ($n \geq 8$) and (**C**) 6 months ($n \geq 9$) after AdCre administration . $^*P > 0.05$ by unpaired, 2-tailed t test.

with urethane (Figure 2C) was RT-PCR amplified and subjected to massively parallel sequencing using the Ion Torrent PGM platform. Based on a minimum of 100 independent sequence reads of each allele, we detected a Q61R mutation in the 129-$Kras^{nat}$ allele in the majority (57%) of tumors from $Kras^{nat/nat}$ *CMV-Cre* mice. Again, we found that the 129-$Kras^{ex3op}$ allele was mutated in only one-third of the tumors arising in $Kras^{ex3op2/nat}$ *CMV-Cre* mice, and only G12D mutations were recovered (Figure 4C and Supplemental Table 5). Thus, we detected fewer and different oncogenic mutations in the $Kras^{ex3op}$ allele of urethane-induced tumors.

Dose-dependent changes are observed with the $Kras^{ex3op}$ *allele.* The above approach permitted a detailed analysis of the relative mutation frequency of the $Kras^{ex3op}$ allele versus that of the $Kras^{nat}$ allele inherited from the same parental strain, but required the carcinogen to be administered to F1 progeny of a mixed BL6/129 background. This precluded treatment of mice homozygous for the $Kras^{ex3op}$ allele. Thus, we repeated the analysis in a 129 background to assess all possible *Kras* genotypes. Specifically, we crossed 129-$Kras^{ex3op(neo)/nat}$ mice with a 129S/Sv-*PRM-Cre* line that expresses Cre recombinase in the male germline. Male 129-$Kras^{ex3op(neo)/nat}$ *PRM-Cre* offspring were crossed with 129 females to generate progeny with confirmed excision of the *neo* cassette and lacking the *PRM-Cre* transgene. These mice were crossed to populate cohorts of 129-$Kras^{nat/nat}$, $Kras^{ex3op/nat}$, and $Kras^{ex3op/ex3op}$ littermates, which were injected with urethane, as above, to induce lung tumors (Figure 5A). Since the 129 strain is more permissive of tumor formation (22), lungs were removed for analysis 4 months after carcinogen treatment. Again, in this fourth replicate experiment, we observed a greater than 2-fold reduction of tumor burden in 129-$Kras^{ex3op/nat}$ mice compared with that observed in their 129-$Kras^{nat/nat}$ littermates (Figure 5B), which again could be ascribed in large part to a reduction in tumor number rather than tumor size (Supplemental Figure 6A). $Kras^{ex3op/ex3op}$ mice exhibited a nearly 8-fold reduction in tumor burden compared with that seen in 129-$Kras^{nat/nat}$ littermates at this time point, with most animals having no tumors (Figure 5B). To determine whether tumor formation was delayed or initiation was unsuccessful in 129-$Kras^{ex3op/ex3op}$ mice, we assessed a larger cohort and a later time point. While both 129-$Kras^{ex3op/ex3op}$ and 129-$Kras^{nat/nat}$ mice had increased tumor burden 6 months after urethane administration, more than half of the 129-$Kras^{ex3op/ex3op}$ mice remained tumor free, exhibiting a 6-fold overall reduction in tumor burden (Figure 5C and Supplemental Figure 6B). These results suggest that the $Kras^{ex3op}$ allele inhibits lung tumorigenesis in a dose-dependent manner.

To assess the mutational status of the *Kras* genes in this background, we subjected RT-PCR–amplified *Kras* mRNA from tumors to massively parallel sequencing on the Ion Torrent PGM platform, as above. Again, we found that nearly three-quarters of the tumors from 129-$Kras^{nat/nat}$ mice contained a Q61L/R mutation. In contrast, we detected no oncogenic mutations in the $Kras^{ex3op}$ allele in tumors from the 129-$Kras^{ex3op/nat}$ mice. Instead, oncogenic mutations were only detected in the $Kras^{nat}$ allele and occurred at codon 61. Last, while few tumors developed in $Kras^{ex3op/ex3op}$ mice, tumors that did develop usually lacked a detectable oncogenic mutation in *Kras*. Moreover, when a mutation was detected, it was either G12D or Q61R (Figure 5D and Supplemental Table 6). Thus, tumor development is sensitive to the dose of the $Kras^{ex3op}$ allele.

Oncogenic mutation of $Kras^{ex3op}$ *potentiates downstream signaling.* Oncogenic *Kras* mutations detected in tumors after urethane administration are considered driver mutations (21). We found that altering *Kras* codon bias predominantly affected tumor initiation, as tumor number rather than size was primarily reduced in the presence of the $Kras^{ex3op}$ allele (Supplemental Figures 3 and 6). KRAS protein levels were elevated in the $Kras^{ex3op/ex3op}$ background (Figure 1, G and H), and high levels of transgenic $HRAS^{G12V}$ have been shown to induce widespread senescence in the mouse mammary gland in vivo (10). Furthermore, converting rare codons into common codons in *KRAS* suppressed cell proliferation of normal cells (4). Thus, higher protein levels from the $Kras^{ex3op}$ allele may increase the chance that an oncogenic mutation will result in growth arrest, accounting for the reduced number of tumors in $Kras^{ex3op/nat}$ mice injected with urethane.

To assess the response of normal cells to oncogenic codon–altered *Kras*, each of the oncogenic *Kras* mutations recovered from urethane-induced lung tumors, namely, G12V, G12D, Q61L, and Q61R, were introduced into FLAG epitope–tagged *nat* or *ex3op* *Kras* cDNAs. The human lung fibroblast cell line IMR90, which undergoes growth arrest upon expression of oncogenic *HRAS* (23), was stably infected with retroviruses encoding no oncogene as a negative control (empty), $FLAG\text{-}HRAS^{G12V}$ as a positive control, or either *FLAG-*$Kras^{nat}$ or *FLAG-*$Kras^{ex3op}$ with 1 of the 4

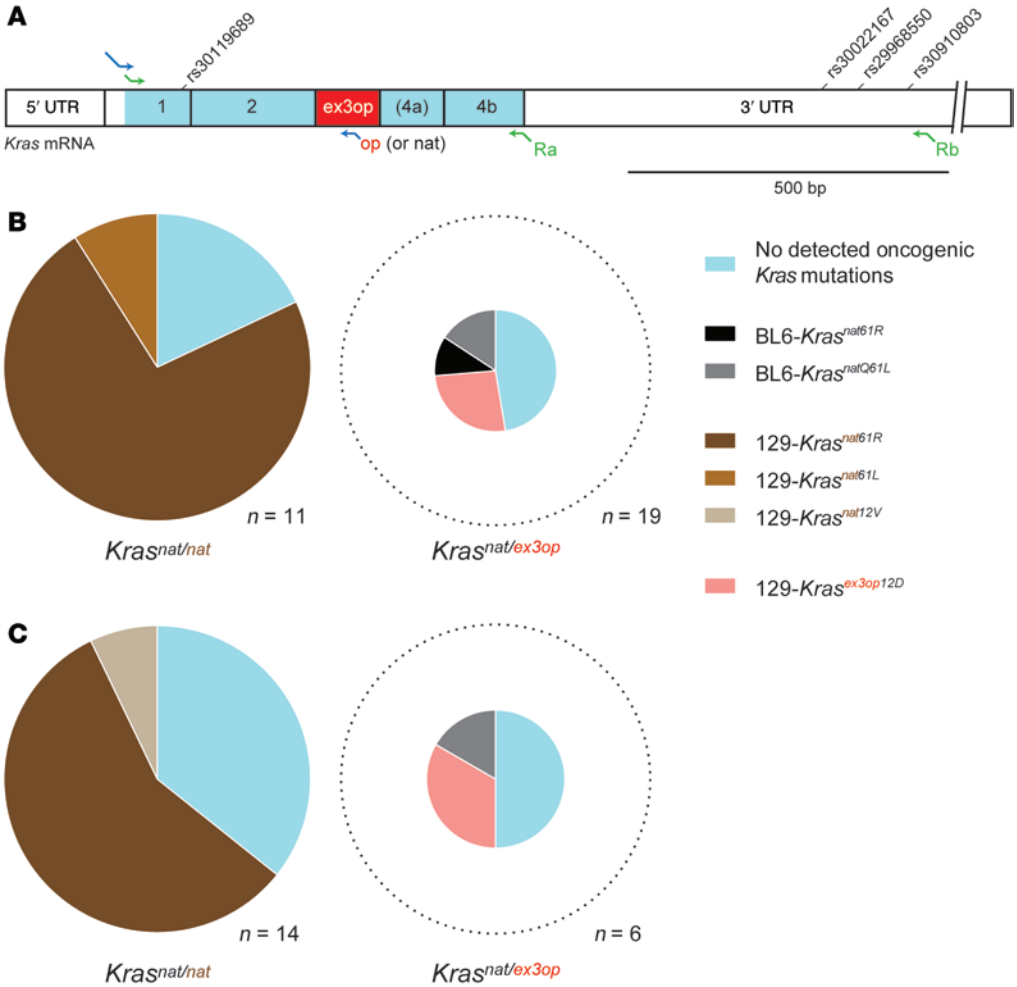

Figure 4. Detection of fewer and different mutations in the *Kras*^{ex3op} allele from tumors of mice treated with urethane. (**A**) Amplification strategy for *Kras* RT-PCR including location of SNPs used for strain identification. Green arrows indicate primers for Sanger sequencing; blue arrows indicate primers for Ion Torrent sequencing. (**B** and **C**) Sequencing by the (**B**) Sanger and (**C**) Ion Torrent methods of *Kras* cDNAs from the indicated number (*n*) of tumors arising in the indicated urethane-treated cohorts revealed fewer and different mutations in the *Kras*^{ex3op} allele. Pie charts are sized to reflect differences in overall tumor multiplicity for each genotype.

aforementioned oncogenic mutations. Immunoblot analysis revealed the expected robust expression of FLAG-HRAS^{G12V} (4) and higher expression of FLAG-KRAS in cells transduced with oncogenic *FLAG-Kras*^{ex3op} transgenes compared with those transduced with the *FLAG-Kras*^{nat} counterparts with the same oncogenic mutations. In agreement with these findings, we found that phosphorylated (T202/4) ERK1/2 (p-ERK), a measure of oncogenic RAS activation of the MAPK pathway, was also slightly elevated in cells transduced with *FLAG-Kras*^{ex3op} compared with those transduced with *FLAG-Kras*^{nat} oncogenes (Figure 6A). Thus, conversion of rare codons into common ones increases ectopic KRAS protein expression and downstream MAPK signaling.

A comparison between Q61L/R and G12V/D mutations in the FLAG-KRAS protein revealed that expression levels of the former mutant were unexpectedly higher and correspondingly stimulated the MAPK pathway to a greater degree, as assessed by p-ERK levels. The difference between these mutants was observed in both the *nat* and *ex3op* versions of FLAG-KRAS, although the effect was more pronounced in the *FLAG-Kras*^{ex3op} lines (Figure 6A). These mutations are structurally and biochemically distinct. Q61 mutations alter a coordinating catalytic amino acid (24, 25), while G12 mutations sterically inhibit the arrangement of GAP and RAS-Q61 residues critical for GTP hydrolysis (26). In general agreement with this, pull-down of RAS with the RAF1 RAS–binding domain (RBD) revealed higher levels of GTP-bound KRAS from cells transduced with *FLAG-Kras*^{ex3op} than were detected from matched *FLAG-Kras*^{nat}–transduced cells and, at least in the case of Q61R, higher levels of GTP-bound KRAS than were detected with G12V/D mutants (Supplemental Figure 7). Thus, oncogenic mutations in *Kras*^{ex3op} and Q61L/R mutations are comparatively more potent than oncogenic mutations in *Kras*^{nat} and G12V/D mutations, respectively, as assessed by KRAS-GTP and p-ERK levels. These results suggest that the most potent oncogenic combination is that of Q61L/R mutations in the *Kras*^{ex3op} codon–optimized version of *Kras*.

Oncogenic Kras^{ex3op} *suppresses cell proliferation*. Growth arrest in response to oncogenic stress induced by oncogenic RAS is largely attributed to stimulation of the MAPK pathway (9). Immunoblot analysis revealed that expression of FLAG-*Kras*^{ex3op} with Q61L/R oncogenic mutations led to the highest level of MAPK activation (Figure 6A). Consistent with this, only expression of FLAG-*Kras*^{ex3op} with a Q61L/R oncogenic mutation induced upregulation of p16 (Figure 6A), a marker of cellular senescence (23). Q61L/R mutations in *Kras*^{ex3op} were also very rarely recovered from urethane-induced tumors. One explanation for the observed reduction in tumor burden and mutations recovered from the *Kras*^{ex3op} allele is that Q61L/R mutations, in the context of a codon-optimized exon 3 transcript, result in higher levels of activated KRAS that mediate growth arrest and hence are rarely detected.

To explore this hypothesis, the above primary lung fibroblasts were stably transduced with *HRAS*^{G12V} and the different mutant versions of *Kras*^{nat} and *Kras*^{ex3op} (Figure 6A). We calculated cell doublings when the vector control cells approached confluence. As expected (4, 23), cells expressing *HRAS*^{G12V} exhibited a pronounced

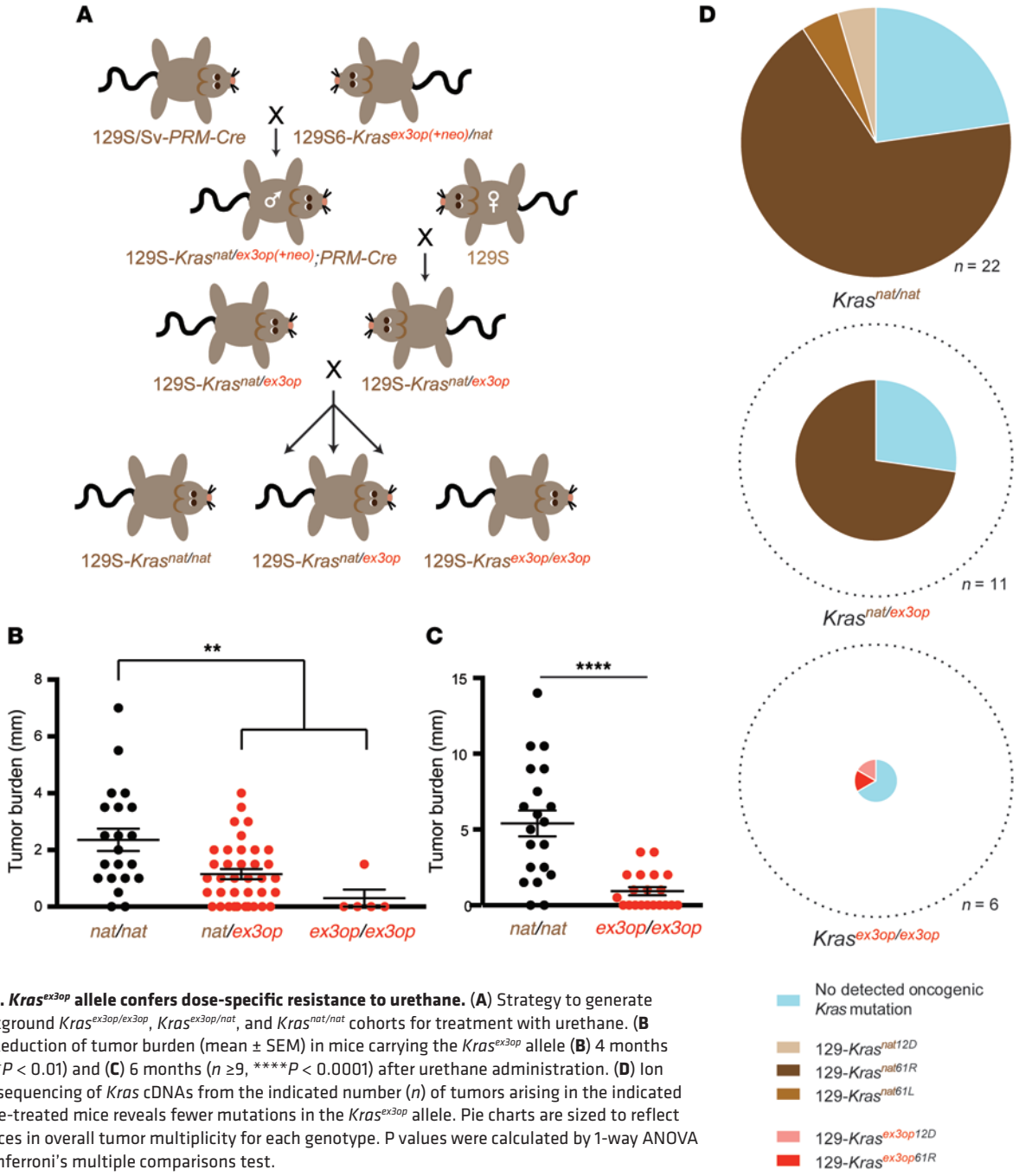

Figure 5. *Kras*^{ex3op} allele confers dose-specific resistance to urethane. (**A**) Strategy to generate 129 background *Kras*$^{ex3op/ex3op}$, *Kras*$^{ex3op/nat}$, and *Kras*$^{nat/nat}$ cohorts for treatment with urethane. (**B** and **C**) Reduction of tumor burden (mean ± SEM) in mice carrying the *Kras*^{ex3op} allele (**B**) 4 months ($n \geq 5$, $^{**}P < 0.01$) and (**C**) 6 months ($n \geq 9$, $^{****}P < 0.0001$) after urethane administration. (**D**) Ion Torrent sequencing of *Kras* cDNAs from the indicated number (n) of tumors arising in the indicated urethane-treated mice reveals fewer mutations in the *Kras*^{ex3op} allele. Pie charts are sized to reflect differences in overall tumor multiplicity for each genotype. P values were calculated by 1-way ANOVA with Bonferroni's multiple comparisons test.

growth arrest compared with that observed in vector control cells. Consistent with the immunoblot analysis, Q61L/R mutations in *Kras*^{nat} suppressed cell proliferation more than did G12V/D mutations. We observed a similar trend with *Kras*^{ex3op} oncogenes. Additionally, expression of *Kras*^{ex3op} with 3 of the 4 oncogenic mutants suppressed proliferation to a greater degree than did corresponding *Kras*^{nat} oncogenes, although the difference only reached statistical significance in 1 comparison (Figure 6B). To independently assess whether the differences observed in growth arrest were attributable to altered codon bias, we synthesized completely artificial *Kras* cDNAs using all common codons (*Kras*^{common}) or all rare codons (*Kras*^{rare}). We found that expressing *Kras*^{common} in either the G12D- or Q61R-mutant configuration suppressed cell proliferation to a greater degree than did *Kras*^{rare} with the same oncogenic mutations (Figure 6C). Thus, *Kras* oncogenes enriched by common codons more potently suppress proliferation of primary cells.

A Cdkn2a-null background blunts Kras^{ex3op} *inhibition of lung tumor initiation.* Based on the above results, oncogenic mutations in the *Kras*^{ex3op} allele may lead to growth arrest, thereby accounting for the reduced tumor burden in *Kras*^{ex3op} mice injected with urethane. Expression of oncogenic *Kras* in mouse lungs induces p16^{INK4A} expression and a senescent growth arrest (27). Disruption of the *Cdkn2a* locus encoding p16^{INK4A} and p19^{ARF} is known to partially suppress *Ras* oncogene–induced senescence (28–30) and

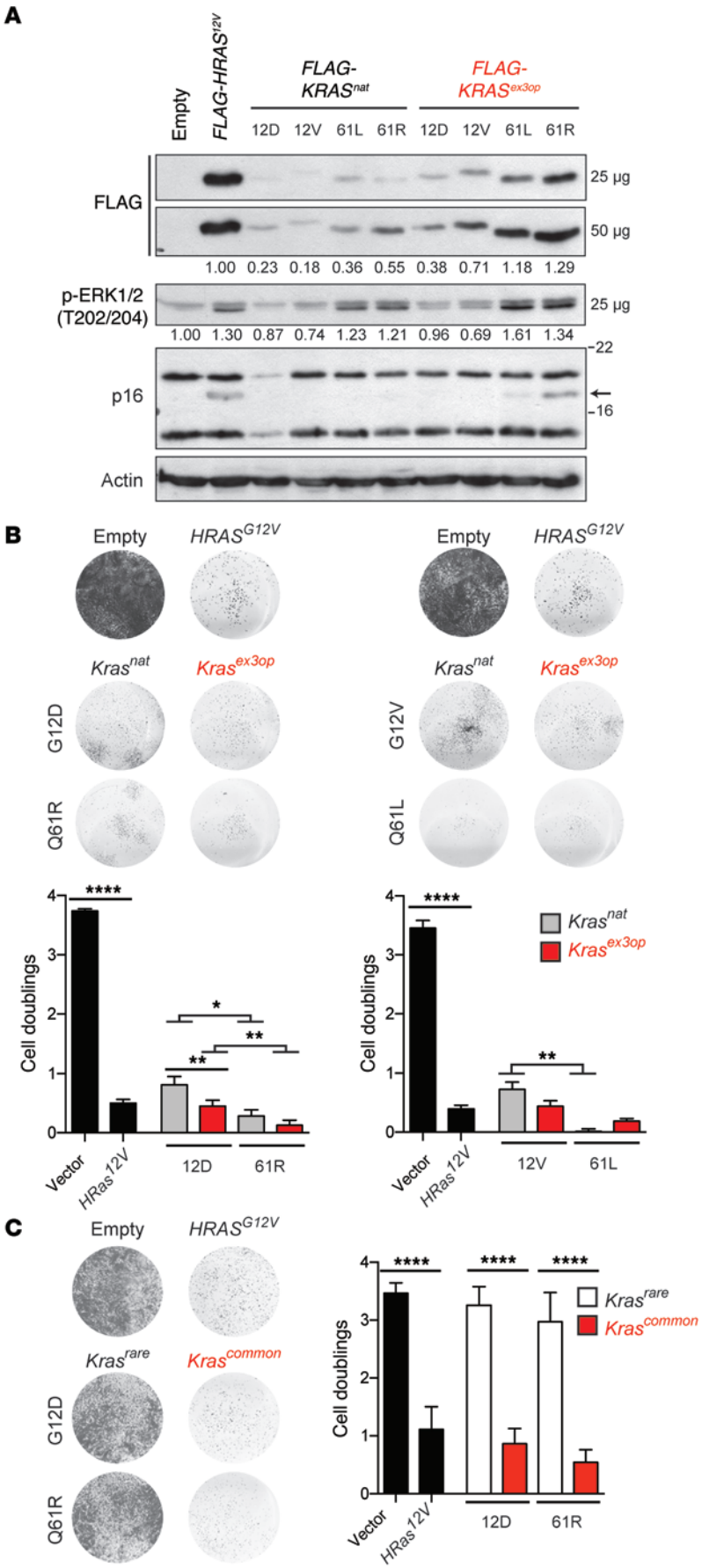

Figure 6. Q61 oncogenic mutations in *Kras*^{ex3op} induce growth arrest in normal cells. (**A**) Immunoblots revealed that oncogenic Q61L/R mutations in Kras^{ex3op} induced the highest levels of p-ERK1/2 and p16 (indicated with an arrow) in primary human lung fibroblasts. Quantifications of FLAG-tagged constructs are normalized to FLAG-HRAS^{G12V}. Quantifications of p-ERK1/2 were normalized to empty vector control. (**B** and **C**) Images and mean ± SEM of primary human lung fibroblast growth arrest in response to (**B**) the indicated *Kras* oncogenes and (**C**) *Kras*^{common} and *Kras*^{rare} oncogenes (1 of at least 2 experiments using independently derived cell lines). Images are of individual wells from 6-well plates. $^{*}P < 0.05$, $^{**}P < 0.01$, $^{****}P < 0.0001$, by repeated-measures 1-way ANOVA with Bonferroni's multiple comparisons test.

permits sustained MAPK signaling and tumor progression in an oncogenic *Kras*–driven mouse model of lung cancer (31). Hence, suppressing the ability of normal cells to respond to oncogenic stress vis-à-vis disruption of the *Cdkn2a* locus may permit oncogenic mutations in the *Kras*^{ex3op} allele to be better tolerated.

To test the effect of a *Cdkn2a*-null background on urethane-induced lung tumorigenesis in mice with *nat* or *ex3op Kras* alleles, *Kras*$^{ex3op/nat}$ *Cdkn2a*$^{+/-}$ mice were crossed to populate cohorts of *Kras*$^{nat/nat}$, *Kras*$^{ex3op/nat}$, and *Kras*$^{ex3op/ex3op}$ littermates that were either *Cdkn2a*$^{-/-}$ or *Cdkn2a*$^{+/+}$ (Figure 7A). Mice were administered urethane and assessed for lung tumor burden 2.5–3 months later for *Cdkn2a*$^{-/-}$ cohorts and 4 months later for *Cdkn2a*$^{+/+}$ cohorts. Early assessment of lung lesions was necessary in the *Cdkn2a*$^{-/-}$ cohorts due to accelerated moribundity not associated with lung tumor burden (data not shown). While the overall incidence of lung lesions at this early time point was low, we found no statistical difference in tumor number, size, or burden between the 3 *Kras* genotypes (Figure 7, B–D). In fact, there instead appeared to be a trend toward increased tumor size in *Kras*$^{ex3op/ex3op}$ mice, which we did not observe in *Cdkn2a*$^{+/+}$ mice (Figure 7D and Supplemental Figure 8C). These tumors were the result of urethane carcinogenesis, as no lung lesions were detected in any untreated *Cdkn2a*$^{-/-}$ cohorts at this time point (data not shown). Furthermore, we found that matched *Cdkn2a*$^{+/+}$ littermates retained significant differences in tumor burden between *Kras* genotypes, as observed in previous experiments (Supplemental Figure 8). Thus, a *Cdkn2a*$^{-/-}$ background dampens the differences in tumor initiation between *Kras*$^{nat/nat}$, *Kras*$^{ex3op/nat}$, and *Kras*$^{nat/nat}$ mice injected with urethane.

Discussion

It is well appreciated that protein expression is affected by codon bias in heterologous systems (7). There is also emerging evidence that rare codons within mammalian genes can have biochemical or cellular consequences (4, 32–35). We now show that

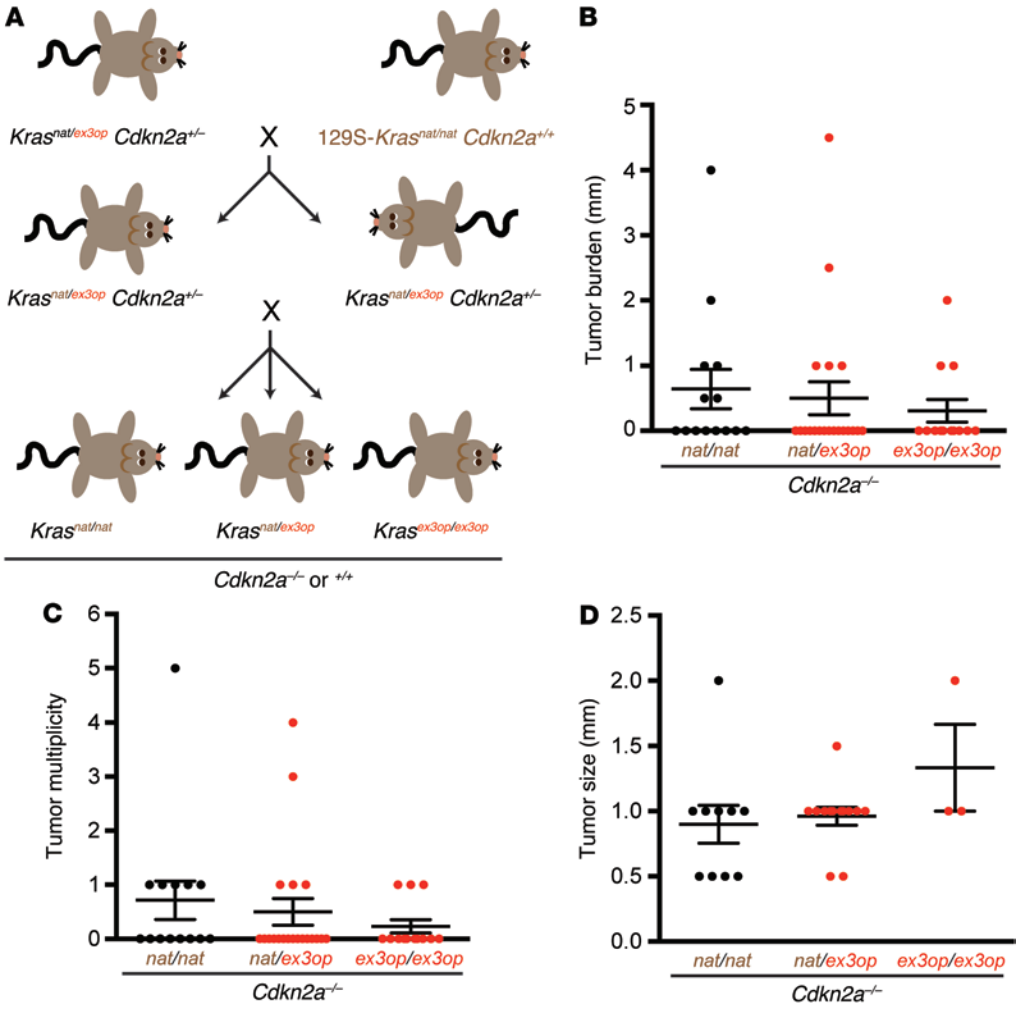

Figure 7. Reduced urethane tumor initiation imparted by the *Kras*^{ex3op} allele is blunted in a *Cdkn2a*$^{-/-}$ background. (**A**) Strategy to generate *Cdkn2a*$^{-/-}$ and *Cdkn2a*$^{+/+}$ littermates with *Kras*$^{ex3op/ex3op}$, *Kras*$^{ex3op/nat}$, and *Kras*$^{nat/nat}$ genotypes for urethane carcinogenesis. (**B**) Similar tumor burden ($P = 0.69$), (**C**) number ($P = 0.49$), and (**D**) size ($P = 0.23$) between *Kras* genotypes (mean ± SEM) in the context of a *Cdkn2a*$^{-/-}$ background, as assessed 2.5–3 months after urethane administration ($n \geq 13$). P values were calculated by 1-way ANOVA with Bonferroni's multiple comparisons test.

altering codon bias has a biological impact on the function of an endogenous mammalian gene in vivo. Specifically, the 3 genes of the mammalian *RAS* family display different codon usage, with *Kras* having the most rare codons (Figure 1C and ref. 4). Converting 27 rare codons to common codons in exon 3 of *Kras* renders mice more resistant to urethane-induced carcinogenesis. Given the prevalence of rare codons in many other genes as well as the divergent codon usage between numerous highly similar gene pairs (4), codon bias may similarly underlie previously unappreciated functional aspects of other mammalian genes.

Mechanistically, the reduction of urethane-induced carcinogenesis upon conversion of rare *Kras* codons into common codons involves both alleles of *Kras*. With regard to the oncogenic *Kras* allele, accumulating evidence suggests that high levels of oncogenic RAS induce a senescent growth arrest instead of proliferation (9). We now demonstrate that expressing oncogenic *Kras*^{ex3op} results in an increase in total and GTP-bound KRAS and MAPK signaling, which in turn more potently suppresses proliferation of primary lung fibroblasts. Furthermore, we show that the *Kras*^{ex3op} gene also yields higher protein levels and reduced tumor burden in mice injected with urethane. Admittedly, these effects could be the product of other features intrinsic to the *Kras* locus altered by the targeting strategy (12, 13, 19, 36) or other unknown effects of altering rare codons. However, the parsimonious nature of changes to the *Kras* locus and the consistent phenotype of the *Kras*^{ex3op} oncogenes in an independent, cell-based assay are supportive of a model in which oncogenic mutations in the *Kras*^{ex3op} allele are selected against due to higher protein expression inducing growth arrest instead of proliferation. Extending these results one step further, we speculate that poor expression imposed by rare codons may increase the likelihood that an oncogenic mutation in *KRAS* will lead to proliferation instead of growth arrest, which may account for the high frequency of mutations in *KRAS* compared with those occurring in the other *RAS* genes in human cancers (1, 2). Paradoxically, rare codons hamper the oncogenic activity of KRAS in cells resistant to oncogene-induced stress (4). As such, we speculate that the rare codon bias of oncogenic *KRAS* poses a barrier to more malignant phenotypes once cells overcome oncogene-induced stress, which may lead to the selection of mechanisms to increase RAS signaling.

With regard to the nononcogenic *Kras* allele, decreased *Kras* gene dosage increases sensitivity to urethane carcinogenesis, indicative of a tumor-suppressive role for the WT *Kras* allele (18). In agreement with this finding, we now show that the converse is true, namely, that converting rare codons into common codons in the nononcogenic *Kras* allele, which can elevate protein expression, reduces tumor burden when the opposing allele is oncogenic. WT RAS proteins can also promote tumor growth through a variety of mechanisms, including enhancing signaling (37–39), suppressing apoptosis (40, 41), and modulating a DNA damage response (42). Since these tumor-promoting effects were elucidated in established cancer cell lines that are typically resistant to oncogene-induced stress, it stands to reason that the nononcogenic *Kras*^{ex3op} allele similarly promotes tumorigenesis in more malignant cells,

although this remains to be tested. As such, the contribution of WT RAS proteins to signaling may be tumor suppressive during tumor initiation, at least in some settings, but tumor promoting once tumor cells become insensitive to oncogene-induced stress.

The observed shift from Q61L/R to G12V/D mutations in the $Kras^{ex3op}$ allele in the tumors of some strain backgrounds after urethane administration may also be related to oncogenic potency. Q61L/R mutations appeared more active than G12V/D mutations in vitro and resulted in more potent growth arrest of primary lung fibroblasts. In fact, Q61L/R mutations in $Kras^{ex3op}$ were the only *Kras* oncogenes that induced detectable p16 expression. These mutations were very rarely detected in the $Kras^{ex3op}$ allele of lung tumors. This raises the intriguing possibility that the ostensibly more potent Q61L/R mutations were selected against in the more highly expressed $Kras^{ex3op}$ allele, perhaps in favor of the apparently weaker G12V/D mutations, which may evade a growth-arrest response. On the other hand, G12V/D mutations are normally rarely detected in the *Kras* allele of lung tumors developing after administration of urethane. Thus, these mutations may be too weak to promote tumorigenesis from a native *Kras* allele, hence the common detection of Q61L/R mutations in urethane-induced lung tumors. In agreement with these findings, it was recently reported that $NRAS^{Q61R}$, but not $NRAS^{G12D}$, promotes melanomagenesis (43). Taken together, these results suggest that there may be a narrow window of oncogenic RAS signaling that may vary by cell type and that can lead to tumorigenesis. It is thus possible that the prevalence of specific *RAS* mutations in different cancers (1, 2) are related, in some measure, to the magnitude of oncogenic signaling imparted by the mutation.

In conclusion, we demonstrate that there is a phenotypic consequence of altering rare codons in a proto-oncogene, establishing a role for this previously unappreciated feature of the *Kras* gene in de novo tumorigenesis.

Methods

Generation of codon-altered Kras exon 3 knock-in ($Kras^{ex3op}$) mice. A knock-in construct was created using long and short arms of homology from a 129S7/AB2.2 genomic mouse BAC and a synthetic exon 3, in which all rare codons were converted into 1 of the 2 most commonly used codons in the mouse genome, provided they were not located in annotated or likely sites that would affect splicing of the gene. Targeting of the *Kras* allele in 129S6-Taconic ES cells and blastocyst injection were performed using standard procedures.

Codon usage plots. The codon usage index was calculated according to the method described for the codon adaptation index (44), but with the relative codon frequency derived from codon usage in the mouse exome (6). Values were calculated for sliding windows of 25 codons across each transcript. A theoretical *Kras* transcript encoded by all common (red dotted line) or all rare (black dotted line) codons were plotted for reference (Figure 1C).

Plasmids. FLAG-tagged *RAS* constructs were subcloned into pBabePuro for the generation of retrovirus. FLAG-tagged human *HRAS* and *KRAS* constructs were described previously (37). FLAG-tagged chimeric *KRAS* with exon substitutions were constructed by replacing the indicated exons with *HRAS* codons. FLAG-tagged mouse *Kras4b* cDNAs were subcloned from mouse tumors. Oncogenes not recovered from tumor samples were created using site-directed mutagenesis. $FLAG\text{-}Kras^{common}$ and $FLAG\text{-}Kras^{rare}$ were synthesized by GeneArt Gene synthesis (Invitrogen).

Design of synthetic $Kras^{common}$ and $Kras^{rare}$ sequences. Selection of common and rare codons for $Kras^{common}$ *and* $Kras^{rare}$ cDNAs was done on the basis of annotated codon usage in the mouse exome (6). These cDNAs used entirely rare or common codons with one minor exception. The poly-lysine stretch in the *Kras4b* C terminus (beginning at codon 176) was not fully optimized due to concerns about artifacts resulting from 18 sequential adenines in the rare cDNA (45). Among vertebrate *Kras* transcripts, these lysines are always encoded by a mixture of the more rare (AAA) and more common (AAG) codons, and more than 5 sequential adenines are not observed. Hence, alternating AAA and AAG codons were used in both the $Kras^{common}$ and $Kras^{rare}$ cDNAs.

Semiquantitative Kras RT-PCR. RNA was isolated from MEFs using RNA-Bee (Fisher Scientific). Reverse transcription reactions were primed with Oligo(dT) (Invitrogen) using M-MuLV Reverse Transcriptase (New England Biolabs) with the addition of RNAseOUT (Invitrogen). PCR amplification was performed using Platinum Taq (Invitrogen) polymerase, with the supplied buffer used at 0.7 times the suggested final concentration, 1 mM dNTPs, 2 mM $MgCl_2$, and 0.4 μM forward and reverse primers. Primer sequences are detailed in Supplemental Table 7. Reactions were run using the standard PCR conditions of denaturation at 94°C for 30 seconds, annealing at 50°C for 30 seconds, and elongation at 72°C for 2 minutes. Cycle numbers are indicated on the corresponding figure. Bands were resolved using 2% agarose gel electrophoresis with ethidium bromide staining. Results are representative of comparisons between $Kras^{nat/nat}$ and $Kras^{ex3op/ex3op}$ littermate MEFs derived from 2 litters.

Protein analysis. Whole-cell lysates were prepared from pelleted cultured cells (see below) stored at −80°C until lysed. Lysates from whole lung tissue were prepared by snap freezing, followed by mortar and pestle tissue disruption under liquid nitrogen. RAS-GTP pulldown assays were conducted as previously described using 1 mg total protein (46). Equal protein levels were resolved and immunoblotted with antibodies against the indicated proteins (Figure 1, A, G, and H, Figure 6A, and Supplemental Figure 7), as previously described (47). Briefly, SDS-PAGE was followed by transfer to a PVDF membrane (Millipore), blocking in 5% BSA (Sigma-Aldrich), and immunoblotting with one of the following antibodies diluted, as indicated, in 5% BSA: αKRAS (1:50, SC-30; Santa Cruz Biotechnology Inc.); α-tubulin (1:1,000, TUB2.1; Sigma-Aldrich); β-actin (1:25,000, AC-74; Sigma-Aldrich); αFLAG (1:1,000, M2; Sigma-Aldrich); αp(Thr202/204) ERK1/2 (1:200, E10; Cell Signaling Technology); or αp16 (1:200, G175-405; BD Biosciences). Signal intensity quantified with ImageJ software (NIH) (48) was normalized to loading controls and compiled from at least 2 immunoblots. Endogenous KRAS is reported relative to $Kras^{nat/nat}$ samples, FLAG-tagged oncogenes are reported relative to $HRAS^{12V}$, and p-ERK1/2 is reported relative to empty control.

Cell culture. MEFs were isolated from E13.5 mouse embryos, as previously described (23), and stably infected with a retrovirus derived from pBabeHygro encoding the early region of SV40 (49) and selected with 100 μg/ml hygromycin to establish immortalized cultures. These immortalized MEFs, HEK-HT cells (4), and IMR90 (ATCC) human fetal lung fibroblasts (pd 38-40) were stably infected with retroviruses encoding no transgene or the indicated *Ras* genes, as previously described (49).

RNA isolation and cDNA synthesis from urethane lung tumors. Dissected tumors were homogenized and RNA isolated using RNA-Bee

(Fisher Scientific). Phase-lock heavy gel (Fisher Scientific) maximized recovery. RNA was coprecipitated with Pellet Paint (Novagen) using isopropanol. Maximal RNA volumes were used for reverse transcription (50% of the total reaction volume) with M-MuLV reverse transcriptase (New England Biolabs), according to the manufacturer instructions, with the addition of Oligo(dT) primers and RNAseOUT.

Infusion cloning of Kras amplicons and Sanger sequencing. Primers with cloning adapters were used for PCR amplification of *Kras* (Supplemental Table 7). PCR amplification was performed using Platinum Taq polymerase, with the supplied buffer used at 0.7 times the suggested final concentration, 1 mM dNTPs, 2 mM $MgCl_2$, 0.4 μM forward and reverse primers, and 5% of the total reaction volume contributed by cDNA. Reactions were run for 40 cycles using the following standard conditions: denaturation at 94°C for 30 seconds, annealing at 55°C for 45 seconds, and elongation at 72°C for 2 minutes. Gel-purified PCR products were cloned into pBluescript using In-Fusion HD (Stratagene), transformed into bacteria, and 8–12 Amp^R clones per tumor sequenced using T3 and T7 primers as necessary to achieve insert coverage.

Kras amplification and Ion Torrent PGM sequencing. Primers with Ion Torrent PGM (Invitrogen) adapter sequences and barcodes corresponding to tumor sample and allele amplified (*native* or *ex3op*, Supplemental Table 7) were used for PCR amplification. PCR reactions used Platinum Taq, the supplied buffer (0.7 times final concentration), 1 mM dNTPs, 1 mM $MgCl_2$, 0.4 μM primers, and 5% of the total reaction volume contributed by cDNA. Reactions were run for 40 cycles as follows: denaturation at 94°C for 30 seconds, step-down annealing at 65°C to 50°C for 45 seconds, and elongation at 72°C for 2 minutes. 450-bp products were gel purified and pooled for sequencing. Sequencing reads were filtered to ensure high quality at the G12 codon, Q61 codon, and *Kras*-coding SNP. Usable reads were defined as exactly matching the consensus 4-bp region surrounding the G12 codon, Q61 codon, and *Kras*-coding SNP. Tumor sample datasets with at least 100 usable reads (representing >58% of total reads) or at least 600 usable reads (representing >45% of total reads) were evaluated for mutations. For these datasets, the 3-bp G12 and Q61 codon sequences and SNP were extracted from each usable read, and total counts for every observed G12, Q61, and SNP combination were quantified. For datasets derived from mixed-background $Kras^{nat/nat}$ mouse tumors, strain alleles were considered adequately sampled if representing greater than 16% of the usable reads in the dataset. Additionally, oncogenic mutations were called if they represented greater than 16% of the usable reads for a given allele (based on the frequency of detection in Sanger analysis). To ensure that mutations were limited to the G12 codon, Q61 codon, and *Kras* coding SNP, all reads passing the above filter were aligned to the *Kras* coding reference sequence spanning exons 1–3 using Bowtie2 and the following alignment parameters: -k 1 –N 1 –L 32 --local. Overall, we detected no other sequence differences within the first 200 bp (corresponding to the upper limit of accurate read sequencing via Ion Torrent) of the *Kras* cDNA. All genomic data are available in the NCBI's SRA data repository (SRP041810).

Growth arrest of primary human cells. As previously described (23), IMR90 cells (pd 35-37) were infected with retroviruses derived from pBabePuro with no insert or the indicated *HRAS* or *Kras* oncogenes, selected with 2 μg/ml puromycin, and plated at 4,000 cells per well in 24-well dishes. On the indicated days, cells were fixed with 10% formalin and stained with 0.1% crystal violet (Sigma-Aldrich). For quantification, crystal violet was extracted with 10% acetic acid, and absorbance at 600 nm was normalized to day 1. Each comparison was performed at least twice, and each sample was evaluated at least in triplicate.

Animal studies. C57BL6/J-*CMV-Cre* (50) and 129S/Sv-*Prm-Cre* (51) mice were obtained from The Jackson Laboratory. $Kras^{ex3op}$ chimeras were crossed with 129S6 mice and progeny screened for germline transmission by genotyping PCR (Supplemental Table 7). Following germline transmission, 129S6-$Kras^{ex3op(+neo)}$ mice were crossed with either B6.C-Tg(CMV-Cre)1Cgn/J or 129S/Sv-Tg(Prm-cre)58Og/J mice, resulting in Cre-mediated excision of the *neo* cassette. Specific strains used for each experiment are detailed within the figures for clarity. Cohorts of mixed-background $Kras^{ex3op/ex3op}$ ($n = 15$) and littermate $Kras^{nat/nat}$ ($n = 6$) mice were monitored for over 18 months to evaluate for the development of abnormal phenotypes. $Hras^{-/-}$ and $Nras^{-/-}$ mice obtained from the National Cancer Institute (NCI) (52) were bred with $Kras^{ex3op}$ mice for assessment of progeny ratios. Pups were visually assessed for chylous ascites (14) between 3 and 8 days of age, followed by genotyping. $CDKN2a^{fl/fl}$ mice (53) were provided by Ron DePinho (Department of Cancer Biology, Division of Basic Science Research, The University of Texas MD Anderson Cancer Center, Houston, Texas, USA) and crossed with mice carrying the *CMV-Cre* transgene to generate whole-animal knockouts to cross with $Kras^{ex3op}$ mice.

Urethane carcinogenesis. Six- to 8-week-old mice were injected i.p. with urethane as previously described (18) and euthanized at the indicated time points indicated in Figures 2, 3, 5, and 7. Lung tumors were counted, measured, dissected and preserved in RNAlater (QIAGEN) or snap frozen in liquid nitrogen for sequencing analysis. Tumor burden was calculated as the sum of tumor diameters (mm). A subset of left lungs were fixed for histologic analysis.

Statistics. Statistical analyses were performed using GraphPad Prism software, version 6 (GraphPad Software). Unpaired, 2-tailed *t* tests with a 95% CI were used for 2-group comparisons. One-way ANOVA with Bonferroni's multiple comparisons test with a single pooled variance and a 95% CI were used for experiments with more than 2 groups. Reported *P* values are adjusted to account for multiple comparisons. A χ^2 test was used for analysis of progeny ratios in breeding experiments. A *P* value of less than 0.05 was considered statistically significant.

Study approval. All mouse care and experiments were performed in accordance with protocols approved by the IACUC of Duke University.

Acknowledgments

We thank Meng Meng Xu and Genna Gomes for technical assistance and members of the Counter Laboratory, David Kirsch for advice, and Cheryl Block, Gary Kucera, and the Duke Cancer Institute Transgenic Mouse Facility for generation of mice with the $Kras^{ex3op(neo)}$ allele. This work was supported by NCI grants R01CA154630 and R03CA165927 (to C.M. Counter) and 120222-RSG-11-048-01-DMC (to D.M. MacAlpine).

Address correspondence to: Chris Counter, DUMC-3813, Durham, North Carolina 27710, USA. Phone: 919.684.9890; E-mail: count004@mc.duke.edu.

Benjamin L. Lampson's present address is: Brigham and Women's Hospital, Boston, Massachusetts, USA.

1. Pylayeva-Gupta Y, Grabocka E, Bar-Sagi D. RAS oncogenes: weaving a tumorigenic web. *Nat Rev Cancer*. 2011;11(11):761–774.
2. Stephen AG, Esposito D, Bagni RK, McCormick F. Dragging Ras back in the ring. *Cancer Cell*. 2014;25(3):272–281.
3. Ahearn IM, Haigis K, Bar-Sagi D, Philips MR. Regulating the regulator: post-translational modification of RAS. *Nat Rev Mol Cell Biol*. 2012;13(1):39–51.
4. Lampson BL, et al. Rare codons regulate KRas oncogenesis. *Curr Biol*. 2013;23(1):70–75.
5. Plotkin JB, Kudla G. Synonymous but not the same: the causes and consequences of codon bias. *Nat Rev Genet*. 2011;12(1):32–42.
6. Nakamura Y, Gojobori T, Ikemura T. Codon usage tabulated from international DNA sequence databases: status for the year 2000. *Nucleic Acids Res*. 2000;28(1):292.
7. Zolotukhin S, Potter M, Hauswirth WW, Guy J, Muzyczka N. A "humanized" green fluorescent protein cDNA adapted for high-level expression in mammalian cells. *J Virol*. 1996;70(7):4646–4654.
8. Hense W, et al. Experimentally increased codon bias in the Drosophila Adh gene leads to an increase in larval, but not adult, alcohol dehydrogenase activity. *Genetics*. 2010;184(2):547–555.
9. Collado M, Serrano M. Senescence in tumours: evidence from mice and humans. *Nat Rev Cancer*. 2010;10(1):51–57.
10. Sarkisian CJ, et al. Dose-dependent oncogene-induced senescence in vivo and its evasion during mammary tumorigenesis. *Nat Cell Biol*. 2007;9(5):493–505.
11. Supek F, Miñana B, Valcárcel J, Gabaldón T, Ben Lehner. Synonymous mutations frequently act as driver mutations in human cancers. *Cell*. 2014;156(6):1324–1335.
12. To MD, et al. Kras regulatory elements and exon 4A determine mutation specificity in lung cancer. *Nat Genet*. 2008;40(10):1240–1244.
13. Dassano A, et al. Mouse pulmonary adenoma susceptibility 1 locus is an expression QTL modulating Kras-4A. *PLoS Genet*. 2014;10(4):e1004307.
14. Ichise T, Yoshida N, Ichise H. H-, N- and Kras cooperatively regulate lymphatic vessel growth by modulating VEGFR3 expression in lymphatic endothelial cells in mice. *Development*. 2010;137(6):1003–1013.
15. Horio Y, et al. Ki-ras and p53 mutations are early and late events, respectively, in urethane-induced pulmonary carcinogenesis in A/J mice. *Mol Carcinog*. 1996;17(4):217–223.
16. Dwyer-Nield LD, et al. Epistatic interactions govern chemically-induced lung tumor susceptibility and Kras mutation site in murine C57BL/6J-ChrA/J chromosome substitution strains. *Int J Cancer*. 2010;126(1):125–132.
17. DeNicola GM, et al. Oncogene-induced Nrf2 transcription promotes ROS detoxification and tumorigenesis. *Nature*. 2011;475(7354):106–109.
18. Zhang Z, et al. Wildtype Kras2 can inhibit lung carcinogenesis in mice. *Nat Genet*. 2001;29(1):25–33.
19. To MD, et al. A functional switch from lung cancer resistance to susceptibility at the Pas1 locus in Kras2LA2 mice. *Nat Genet*. 2006;38(8):926–930.
20. Jackson EL, et al. Analysis of lung tumor initiation and progression using conditional expression of oncogenic K-ras. *Genes Dev*. 2001;15(24):3243–3248.
21. Cazorla M, et al. Ki-ras gene mutations and absence of p53 gene mutations in spontaneous and urethane-induced early lung lesions in CBA/J mice. *Mol Carcinog*. 1998;21(4):251–260.
22. Malkinson AM. The genetic basis of susceptibility to lung tumors in mice. *Toxicology*. 1989;54(3):241–271.
23. Serrano M, Lin AW, McCurrach ME, Beach D, Lowe SW. Oncogenic ras provokes premature cell senescence associated with accumulation of p53 and p16INK4a. *Cell*. 1997;88(5):593–602.
24. Buhrman G, Wink G, Mattos C. Transformation efficiency of RasQ61 mutants linked to structural features of the switch regions in the presence of Raf. *Structure*. 2007;15(12):1618–1629.
25. Buhrman G, Holzapfel G, Fetics S, Mattos C. Allosteric modulation of Ras positions Q61 for a direct role in catalysis. *Proc Natl Acad Sci U S A*. 2010;107(11):4931–4936.
26. Scheffzek K, et al. The Ras-RasGAP complex: structural basis for GTPase activation and its loss in oncogenic Ras mutants. *Science*. 1997;277(5324):333–338.
27. Collado M, et al. Tumour biology: Senescence in premalignant tumours. *Nat Cell Biol*. 2005;436(7051):642–642.
28. Serrano M, et al. Role of the INK4a locus in tumor suppression and cell mortality. *Cell*. 1996;85(1):27–37.
29. Sharpless NE, et al. Loss of p16Ink4a with retention of p19Arf predisposes mice to tumorigenesis. *Nature*. 2001;413(6851):86–91.
30. Busch SE, et al. ARF inhibits the growth and malignant progression of non-small-cell lung carcinoma. *Oncogene*. 2014;33(20):2665–2673.
31. Fisher GH, et al. Induction and apoptotic regression of lung adenocarcinomas by regulation of a K-Ras transgene in the presence and absence of tumor suppressor genes. *Genes Dev*. 2001;15(24):3249–3262.
32. Kimchi-Sarfaty C, et al. A "silent" polymorphism in the MDR1 gene changes substrate specificity. *Science*. 2007;315(5811):525–528.
33. Robinson F, Jackson RJ, Smith CWJ. Expression of human nPTB is limited by extreme suboptimal codon content. *PLoS One*. 2008;3(3):e1801.
34. Zhang F, Saha S, Shabalina SA, Kashina A. Differential arginylation of actin isoforms is regulated by coding sequence-dependent degradation. *Science*. 2010;329(5998):1534–1537.
35. Jacobo SMP, DeAngelis MM, Kim IK, Kazlauskas A. Age-related macular degeneration-associated silent polymorphisms in HtrA1 impair its ability to antagonize insulin-like growth factor 1. *Mol Cell Biol*. 2013;33(10):1976–1990.
36. Manenti G, et al. Cis-acting genomic elements of the Pas1 locus control Kras mutability in lung tumors. *Oncogene*. 2008;27(43):5753–5758.
37. Lim K-H, Ancrile BB, Kashatus DF, Counter CM. Tumour maintenance is mediated by eNOS. *Nature*. 2008;452(7187):646–649.
38. Young A, Lou D, McCormick F. Oncogenic and wild-type Ras play divergent roles in the regulation of mitogen-activated protein kinase signaling. *Cancer Discov*. 2012;3(1):112–123.
39. Jeng H-H, Taylor LJ, Bar-Sagi D. Sos-mediated cross-activation of wild-type Ras by oncogenic Ras is essential for tumorigenesis. *Nat Comm*. 2012;3:1168.
40. Matallanas D, et al. Mutant K-Ras activation of the proapoptotic MST2 pathway is antagonized by wild-type K-Ras. *Mol Cell*. 2011;44(6):893–906.
41. Romano D, et al. The differential effects of wild-type and mutated K-Ras on MST2 signaling are determined by K-Ras activation kinetics. *Mol Cell Biol*. 2013;33(9):1859–1868.
42. Grabocka E, et al. Wild-type H- and N-Ras promote mutant K-Ras-driven tumorigenesis by modulating the DNA damage response. *Cancer Cell*. 2014;25(2):243–256.
43. Burd CE, et al. Mutation specific RAS oncogenicity explains N-RAS codon 61 selection in melanoma [published online ahead of print September 24, 2014]. *Cancer Disc*. doi:10.1158/2159-8290. CD-14-0729 .
44. Sharp PM, Li WH. The codon adaptation index- a measure of directional synonymous codon usage bias, and its potential applications. *Nucleic Acids Res*. 1987;15(3):1281–1295.
45. Gu W, et al. Generalized substitution of isoencoding codons shortens the duration of papillomavirus L1 protein expression in transiently gene-transfected keratinocytes due to cell differentiation. *Nucleic Acids Res*. 2007;35(14):4820–4832.
46. de Rooij J, Bos JL. Minimal Ras-binding domain of Raf1 can be used as an activation-specific probe for Ras. *Oncogene*. 1997;14(5):623–625.
47. Kashatus DF, et al. RALA and RALBP1 regulate mitochondrial fission at mitosis. *Nat Cell Biol*. 2011;13(9):1108–1115.
48. Schneider CA, Rasband WS, Eliceiri KW. NIH Image to ImageJ: 25 years of image analysis. *Nat Meth*. 2012;9(7):671–675.
49. O'Hayer KM, Counter CM. A genetically defined normal human somatic cell system to study ras oncogenesis in vivo and in vitro. *Meth Enzymol*. 2006;407:637–647.
50. Schwenk F, Baron U, Rajewsky K. A cre-transgenic mouse strain for the ubiquitous deletion of loxP-flanked gene segments including deletion in germ cells. *Nucleic Acids Res*. 1995;23(24):5080–5081.
51. O'Gorman S, Dagenais NA, Qian M, Marchuk Y. Protamine-Cre recombinase transgenes efficiently recombine target sequences in the male germ line of mice, but not in embryonic stem cells. *Proc Natl Acad Sci U S A*. 1997;94(26):14602–14607.
52. Esteban LM, et al. Targeted genomic disruption of H-ras and N-ras, individually or in combination, reveals the dispensability of both loci for mouse growth and development. *Mol Cell Biol*. 2001;21(5):1444–1452.
53. Aguirre AJ, et al. Activated Kras and Ink4a/Arf deficiency cooperate to produce metastatic pancreatic ductal adenocarcinoma. *Genes Dev*. 2003;17(24):3112–3126.